IEEE 802.11mc Ranging Performance in a Real NLOS Environment

Enrica Zola
Dept. Network Engineering
Universitat Politècnica de Catalunya
(UPC-BarcelonaTECH)
Barcelona, Spain
enrica.zola@upc.edu

Israel Martin-Escalona
Dept. Network Engineering
Universitat Politècnica de Catalunya
(UPC-BarcelonaTECH)
Barcelona, Spain
israel.martin@upc.edu

***Abstract*—Since IEEE 802.11 defined a couple of enhancements that allow accurate time measurements in COTS Wi-Fi devices, the possibility of achieving precise low-cost distance estimations in Wi-Fi has become a reality. However, many sources of error, such as bandwidth limitations of the Wi-Fi signal, limited clock rate in the device, multipath propagation due to the obstacles in the indoor environment, etc., may add noise to the time measurements and therefore distort the estimated ranging. This study aims at covering the gap existing in the literature by assessing the performance of the ranging estimation in real IEEE 802.11mc stations in a typical NLOS environment. The impact on the accuracy is also explored when the station is held in different positions with respect to the floor.**

***Index Terms*—positioning, location, IEEE 802.11mc, Wi-Fi, RTT, ranging error**

I. Introduction

The wide deployment of IEEE 802.11 networks, both indoors and outdoors, makes them especially interesting for positioning purposes. In 2014, the authors in [1] forecasted that Wi-Fi would soon become the easiest-to-use method for positioning, offering a good alternative in terms of accuracy, precision, and cost, compared to similar systems. Also, since currently many buildings already come with an existing Wi-Fi infrastructure, the Wi-Fi technology paves the way for a wide, easy and cheap solution for delivering location based services (LBS) to Wi-Fi users [2].

Several location techniques are available for IEEE 802.11 networks [3] and they can be classified according to the observed data (e.g., signal strength, time, and angle) and the way such location data are turned into the actual position (e.g., triangulation, multilateration, fingerprinting, etc.) [4]. The received signal strength (RSS) reflects the power level of the signal received by a wireless station (STA). As it can be easily and passively measured at any IEEE 802.11 device, the RSS Wi-Fi observable has been so far the most used metric in the literature. Applying a multilateration approach on this metric may lead to inaccurate locations, especially for indoor and crowded scenarios, where the path loss model may not be accurate enough to represent the environment and the non line of sight (NLOS) conditions plus the multipath propagation typically introduce large errors in the estimation [3]. To overcome this problem, Wi-Fi fingerprinting using RSS measurements is often considered because it does not require the line of sight (LOS) and achieves high applicability in complex indoor environments [5]. Despite representing a promising solution, this approach requires a time-consuming task for constructing the radio map necessary for the fingerprinting; moreover, such an RSS database is vulnerable to environmental dynamics [6], thus limiting its deployment at larger scale.

The time ranging approach is based on the concept of inferring the distance between two wireless nodes (e.g., a Wi-Fi node and its access point (AP)), for instance by measuring the round trip time (RTT) of their data exchange; thus, once at least three RTT measurements are collected from different APs, the multilateration approach allows to extract the node's 2D position. As the IEEE 802.11 was conceived as a communication network, it did not account for providing precise positioning from the beginning. The main drawback is that very precise measurements are needed at the physical layer, which would allow to effectively and precisely timestamp the departure and arrival of a 802.11 frame in order to isolate the true RTT in the data exchange process, while filtering out other processing delays (recall that, a delay of 1 μs may translate to an error of 300 m in the estimated distance, thus requiring a precision of few nanoseconds in order to achieve meter-level accuracy). For that, a change in the standard was required. While waiting for such necessary enhancement, researchers proposed software-based solutions that normally required specific hardware [7], [8] to overcome the problem of precisely measuring RTTs. A software based 802.11 RTT-ranging platform was proposed in [9], aimed at being hardware independent; in order to provide accurate RTT measurements, it is necessary to apply filters that properly process the data.

Some years ago, a couple of enhancements were finally

978-1-6654-2854-5/21/$31.00 ©2021 IEEE

proposed to the 802.11 protocol so that it can provide accurate RTT measurements suitable for indoor positioning. Before the 802.11mc amendment was introduced in the 2016 revision of the protocol [10], for a few years only some devices from specific manufacturers included such enhancements. However, positioning capabilities were mostly left aside. The situation changed in 2018, when Google announced the support of positioning through fine time measurement (FTM) in any smartphone running Android 9.0 or later. Other vendors, such as Intel and Cisco, joined the initiative and started to implement this feature in their devices, both Wi-Fi cards and APs. The list of available devices supporting the IEEE 802.11mc feature is growing and growing [11].

The RTT estimation comes with errors that may be due to bandwidth limitations of Wi-Fi signal, limited clock rate of COTS Wi-Fi devices, multipath propagation, oscillators drifts and jitter, etc. [12]. Moreover, this error is propagated when the RTT measurement is converted to a distance. NLOS scenarios often represent the worst conditions in which ranging location systems can run. In [13], the authors propose to identify NLOS measurements and subsequently filter them out before applying the positioning algorithm. Although the experiments reported in [13] were well founded, they involved mostly light NLOS conditions.

The aim of this paper is to assess the ranging estimation performance that RTT measurements taken by a COTS STA in a real indoor environment may achieve when NLOS are naturally present. To this end, four Google APs running Android 9.0 have been placed in the corners of the scenario, and a Google Pixel 3a STA has been mounted on a tripod in order to fix its orientation and its position in the building. The STA repeatedly executes the ranging application in order to collect a number of RTT samples from each AP, covering four different STA orientations and 117 different reference points (RPs) (i.e., predefined points in the building). A similar experiment was performed in a LOS scenario in the same building [4], assessing the impact of different APs. This study extends the previous one by considering a more complex scenario, made of plasterboard partitions, and where concrete and metal obstacles are also present, thus mixing LOS, light and severe NLOS conditions.

The paper is structured as follows. Section II describes the scenario and methodology used for the performance assessment, whose results are presented in Section III. Finally, the main conclusion are drawn in Section IV.

II. Scenario and Methodology

A. Simulation scenario

The aim of this paper is assessing the actual ranging error expected from actual IEEE 802.11mc STAs in a realistic indoor scenario. To this end, samples have been collected in one of the floors at our Department, with access to several offices; an elevator and two bathrooms are located in the middle, and two concrete columns are also present, as displayed in Fig. 1. The selected scenario accounts for both LOS and NLOS conditions, thus dealing with a more realistic indoor environment compared to previous analysis in [4] [13] and paving the way for a deeper understanding of the impact of NLOS on the accuracy of the IEEE 802.11mc ranging estimation.

Four APs have been placed in the corners of our scenario, each on a chair at 50 cm height from the ground; they are represented by orange circles in Fig. 1. AP1 and AP3 are on the left side of the picture, at the bottom and top, respectively; similarly, AP2 and AP4 are on the right side, bottom and top, respectively.

The measurement campaign consists of one STA fixed at one of the RPs and measuring the RTT wrt these four APs. A total of 117 RPs have been considered and are shown with blue crosses in Fig. 1. Their locations are not completely symmetric in order to avoid a bias in the result (i.e., similar results for AP1 and AP3, and for AP2 and AP4). Also, at each RP, four batches of measurements have been performed, each with a different STA orientation in order to assess its impact on the accuracy: a) vertical (i.e. 90 degrees w.r.t. the floor and with the back cover facing the AP) and portrait (i.e. the short border of the STA towards the ceiling - referred here as VP); b) vertical and landscape (i.e. the long border of the STA towards the ceiling - referred as VL); c) horizontal (i.e. laying parallel to the floor) and portrait (referred as HP); d) horizontal and landscape (referred as HL). In order to keep the STA still in the right position, a tripod has been used with a height of 1.5 m from the ground, as shown in Fig. 2.

The four APs used are Google WiFi [14], which is one of the most widely used AP that officially supports the technology and which provided more accurate distance estimations in the 5GHz band in our previous study [4]. Only the FCC U-NII-1 (channel 42), with transmit power control (TPC) and addressed to indoors (power limited to 200 mW), is considered in this study. The channel bandwidth is 80 MHz. Regarding the STA, one brand that is certainly known to support the IEEE 802.11mc standard is the Google Pixel [15]. Accordingly, a Pixel 3a, one of the most affordable devices of the Google Pixel portfolio, has been used in this work to assess the ranging error.

B. Methodology

The methodology followed during our experiment can be summarised as follows. The following procedure is repeated for each AP, at each RP, and for the STA in the four orientations.

1) First, the Google Pixel device is mounted on the tripod with one of the four orientations (e.g., HP)

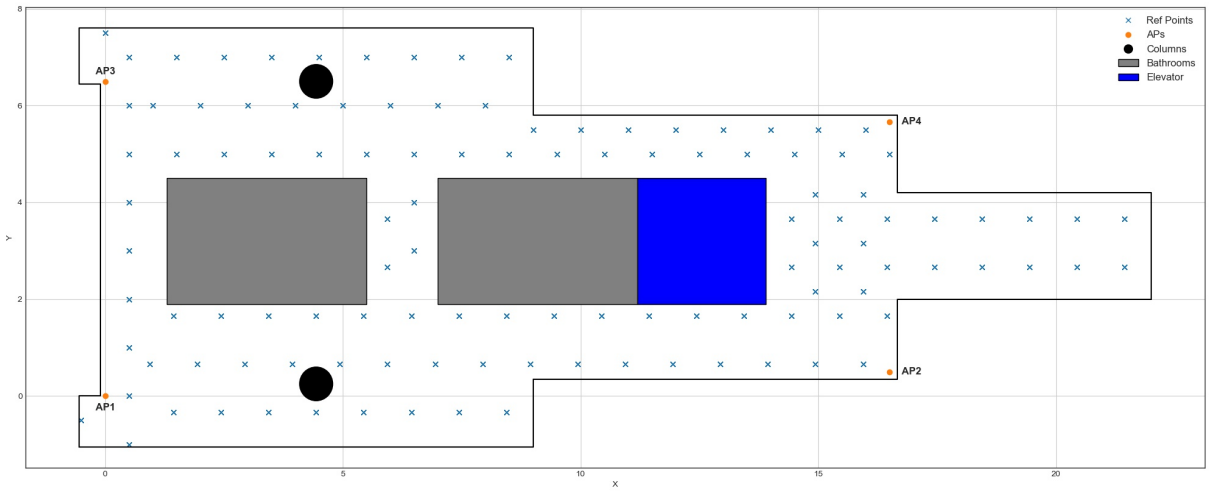

Fig. 1. Performance assessment scenario, consisting of 117 reference points where a STA has been placed to get RTT measurements from four APs. Both LOS and NLOS scenarios are assessed.

Fig. 2. Data collection in the proximity of AP2 and with the STA in vertical and landscape orientation (VL). The reference points are labelled with blue tape on the floor.

and it is located at one RP (one of the blue crosses in the map in Fig. 1)

2) The ranging application is executed, which collects 50 RTT samples from each AP, once at a time (e.g., from AP1 first, then from AP2, AP3 and, finally, from AP4)
3) Once all the APs in the scenario are covered, step 2 is repeated with the STA located in another RP
4) When all the 117 RPs are covered, we go back to step 1 and change the STA orientation

The procedure is ended when the measurement campaign (step1 to step 4) is done for the four STA orientations. All data were collected in the same time slot for approximately one month. We prevented the scenario conditions to change as long as the experiment was conducted (e.g. no people was allowed to walk through corridors while data were gathered).

Every RTT estimation through the Android API involves a single burst consisting of 7 RTT samples (i.e. 8 FTM messages). Once collected, the same API returns the average estimated distance over these 7 RTT samples. In Section III, the 50 samples collected by the Android app for a given set of AP-angle-RP is averaged and, together with other statistics, are considered in order to assess their behavior along different STA orientations and/or for different APs.

III. Results

Figure 3 shows the average estimated RTT distance from each AP and for each STA orientation wrt the actual distance (i.e., Euclidean distance between the RP

TABLE I
MAXIMUM STANDARD DEVIATION OF THE RTT ESTIMATED DISTANCE, FOR EACH AP AND ORIENTATION

Or.:	HP	VP	VL	HL
AP1	[3.46]	[3.65]	[2.58]	[2.39]
AP2	[2.24]	[2.64]	[2.00]	[2.32]
AP3	[4.89]	[4.15]	[2.43]	[2.57]
AP4	[0.66]	[2.48]	[1.62]	[2.74]

TABLE II
PERCENTAGE OF UNDER-2M ERROR FOR EACH AP AND ORIENTATION

Orientation:	HP	VP	VL	HL
AP1	0.6239	0.8376	0.7778	0.7350
AP2	0.3621	0.7350	0.7692	0.6923
AP3	0.5983	0.7692	0.7863	0.7009
AP4	0.4483	0.7521	0.6239	0.6410

and the AP); the bigger the marker, the higher the standard deviation of the estimated distance (see Table I). In general, AP2 (i.e. top-right in Fig. 3) and AP4 (i.e. bottom-right), which in our scenario are located on the right wrt the elevator, show more stable results if compared with those located on the left (i.e., AP1 and AP3). Clear differences also rise depending on the STA orientation, as also observed in the LOS scenario in [4]; this sensitivity to the STA orientation confirms that the consistency of the reported ranges and, consequently, of the computed positions may be compromised.

The maximum standard deviation of the estimated RTT distance is provided in Table I, for each AP and STA orientation. It can be as small as 0.66 (AP4, HP) up to 4.89 (AP3, HP). The minimum standard deviation, instead, ranges between 0.03 and 0.05, being 0.04 for all the AP-RP combinations, except for three. These values help the reader to better understand the magnitudes of the markers in Fig. 3.

The reference distance (blue line) and the 90th percentile (discontinuous gray line) of the overall absolute error are also displayed in Fig. 3. In general, the HP orientation always reports the worst results, with the highest 90th percentile in all the cases (4.64 m). We can observe that, for the two APs placed on the left in our scenario (i.e., AP1 and AP3) and for all the STA orientation except HP, the estimated distance is always negative when the STA is located less than 5 meters away from the AP, as also observed in [4]; this is not always true for the other APs. Finally, AP1 and AP3 always display high dispersion for distances among 13 and 17 meters, for the four STA orientations. This is most probably due to the deep NLOS condition caused by the elevator, as we will discuss later on.

According to [11], the 90% CDF error at the 80MHz bandwidth and in perfect LOS conditions (e.g., large open laboratory without metal objects) should have a tolerance of maximum 2 meters. The 2-meter error band is also depicted in Fig. 3 for this NLOS scenario. The percentage of estimated RTT distances, at each AP and for each STA orientation, with a mean absolute error less than 2 meters is shown in Table II. Again, the HP orientation shows the worst results for all the APs; for the other STA orientations, at least 62.39% of the estimated distances have an error that is lower than 2 m, and it can reach up to 83.76% in some cases. Also, the highest percentages are shown for all the APs when the vertical orientation is used, pointing out that this angle seems to perform better in terms of ranging accuracy.

At a first glance, the spots far away from the reference in Fig. 3 may be assumed as outliers and filtered out. However, it is important to discuss a bit on them. Take the black big spot for AP1 and HP, for instance: it corresponds to RP (15, 5.5) at 15.98 m from AP1 (actual distance) and reports 50 estimated distances that range from 21.8 to 37.78 m, with an average of 36.69 m, a standard deviation of 3.46, and a 90th percentile of 37.72 m. It is thus clear that the RTT measurements gathered in this RP from AP1 suffer the heavy blockage of the elevator, for which the direct path is not sensed at all. The RTT estimations come then after the signal reflects multiple times on the walls; since the measurements are pretty stable, apparently there is one of the multiple paths that is quite strong, thus leading to an overestimate of the distance (e.g., a bias) that is due to the multipath of the NLOS scenario. For this reason, these measurements cannot be easily filtered out; other techniques, as the one presented in [13], should be applied in order to correct the bias.

The 90th percentile of the absolute error, averaged every 1 meter, is shown in Fig. 4 for each STA orientation and AP. Again, the worst results are given in the HP orientation, for all the APs. For the other STA orientations, the 90th percentile of the absolute error is always lower than 2.5 m for actual distances up to 5 m, and it is always lower than 2 m for actual distances between 5 and 10 meters. AP2 (in green) presents the best overall performance, with a 90th percentile error always lower than 2.5 m, except when the STA is held in HP position; in the latter case, there is a peak in the mean absolute error for actual distances of 13 m, which may range up to 7 m for 90% of the measurements.

In general, for actual distances higher than 13 m, the 90th percentile of the absolute error always increases in all the plots in Fig. 4; for AP3 (in cyan), the peak is even more evident for all the STA orientations and for actual distances between 13 and 17 meters, probably corresponding to the points behind the elevator, as it

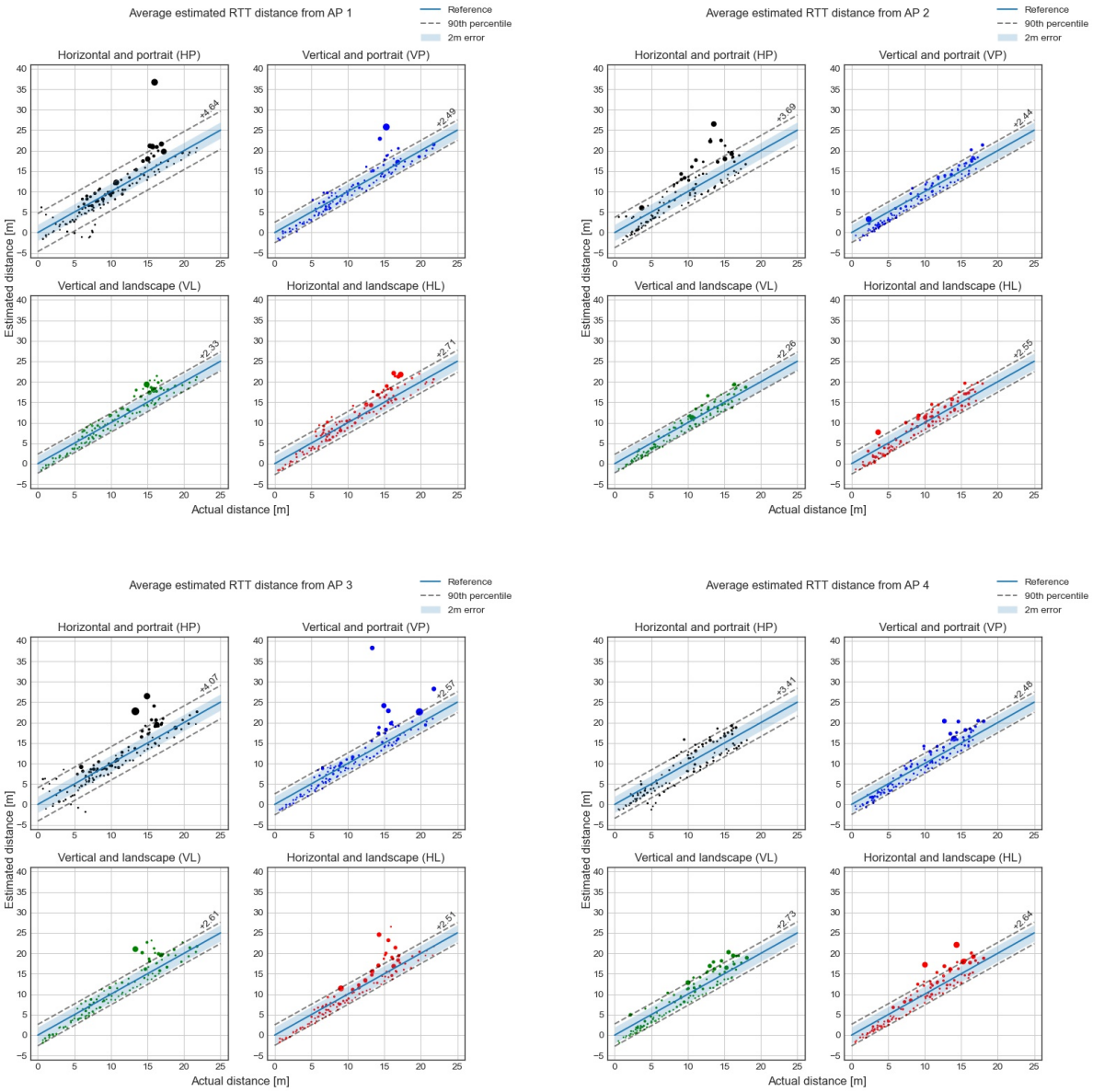

Fig. 3. Average estimated distance versus actual distance (in meters) for AP1 (top-left, a), AP2 (top-right, b), AP3 (bottom-left, c), and AP4 (bottom-right, d), and for the 4 STA orientations, averaged for each actual distance. The bigger the marker the higher the standard deviation of the error. The 90th percentile is displayed in gray, while the 2-meter error in light blue.

will be discussed further in the following paragraph. The asymmetry of the scenario allows for better results for AP1 in this respect (in red). As a general observation, the landscape orientation seems to perform better on the overall.

In order to understand the dependency of the error with the LOS and the NLOS conditions in our scenario, Figures 5(a) to 5(d) draw the error of the estimated distance between a given position in the building and a given AP (i.e., AP1 to AP4, respectively; the AP is represented with a black triangle). The colormap is displayed in logarithmic scale, with dark blue representing an almost zero error, green a 1-meter error, and red an error of 5 meters or higher. First of all, as already observed in [4], due to the calibration algorithm used in the firmware of the devices, the error in the neighborhood of an AP - and in LOS conditions- can be higher than at further distances. Also, we observe smaller errors for points located behind the bathrooms, whose walls are made of plasterboard partitions and thus seem to positively

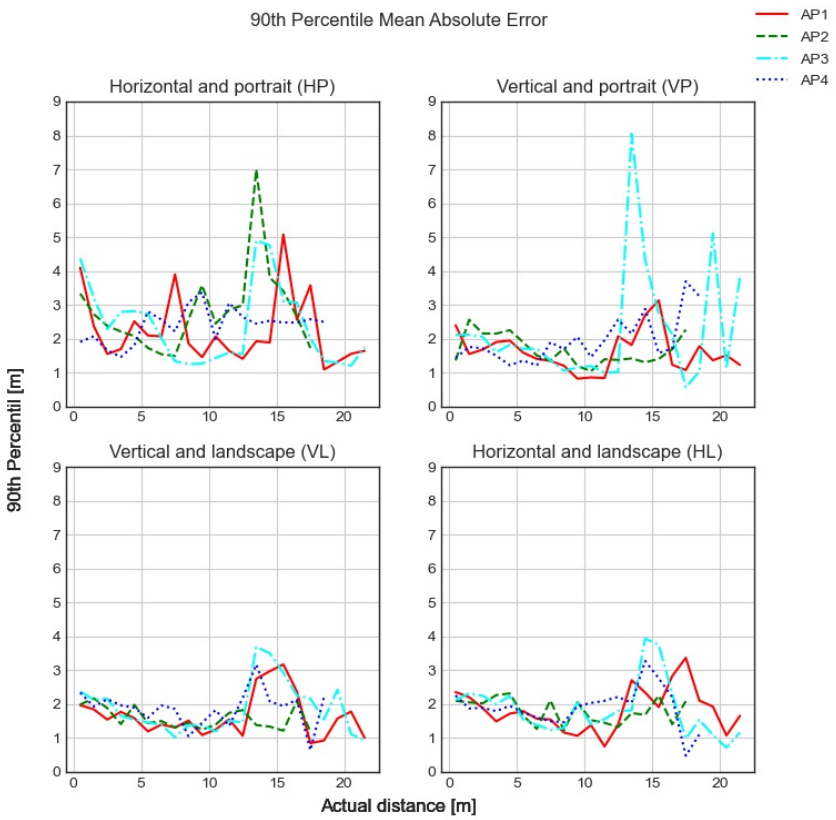

Fig. 4. 90th Percentile of the mean absolute error (averaged at each reference point) for different STA orientations in separated subplot. Different AP are displayed in different colors.

interfere by allowing multiple constructive reflections; this is especially evident for AP1 in Fig. 5(a) and AP3 in 5(c), where larger blue areas are present. A similar trend also appears for the other two APs behind the elevator, probably due to a better geometry that allows for constructive reflections of the signal on the walls; on the other hand, the obstruction caused by the concrete column in the bottom of the figures seems to be especially evident for these two APs. For AP1 and AP3, errors higher than 3 meters rise in the NLOS area behind the elevator, thus confirming that it can constitute a huge blockage for the signal. This behaviour is not present in Fig. 5(b) and 5(d), as again the geometry allows for constructive reflections on the walls. Finally, in the opposite corner where the AP is placed, in LOS with the AP and on the short wall (i.e., in Fig. 5(a) the orange area at $5<y<7$m and $x<1$m, or the orange area in Fig. 5(d) at $14<x<16$m and $y<1$m), again the geometry may favour nonconstructive reflections at the expense of the ranging accuracy.

The probability distribution of the absolute ranging error is displayed in Fig. 6 for the case of distances estimated from the RP at (15, 5.5) to the AP1. This emplacement has been selected due to the noticeable impact of the NLOS on the ranging error, as already commented before. Yet the error distribution noticeably depends on the orientation of the STA, some conclusions can be inferred. Firstly, the absolute ranging error seems to follow a multimodal distribution that seems to consist of several gaussian-like components, as already found in [4]. Secondly, the wider the main component of the error, the more noticeable the modes. Accordingly, the less the standard deviation of the absolute ranging error, the more likely the error follows a unimodal-like distribution. Thirdly, observations are positively or negatively biased depending on the orientation, which means that, in NLOS scenarios, the ranging estimation error is much more sensitive to the reception conditions at the STA than in the case of LOS observed in [4].

IV. Conclusion

The evolution of the ranging error associated to the IEEE 802.11mc FTM scheme [10] has been assessed in a real scenario made of plasterboard partitions, with bathrooms and an elevator in the middle. This study ex-

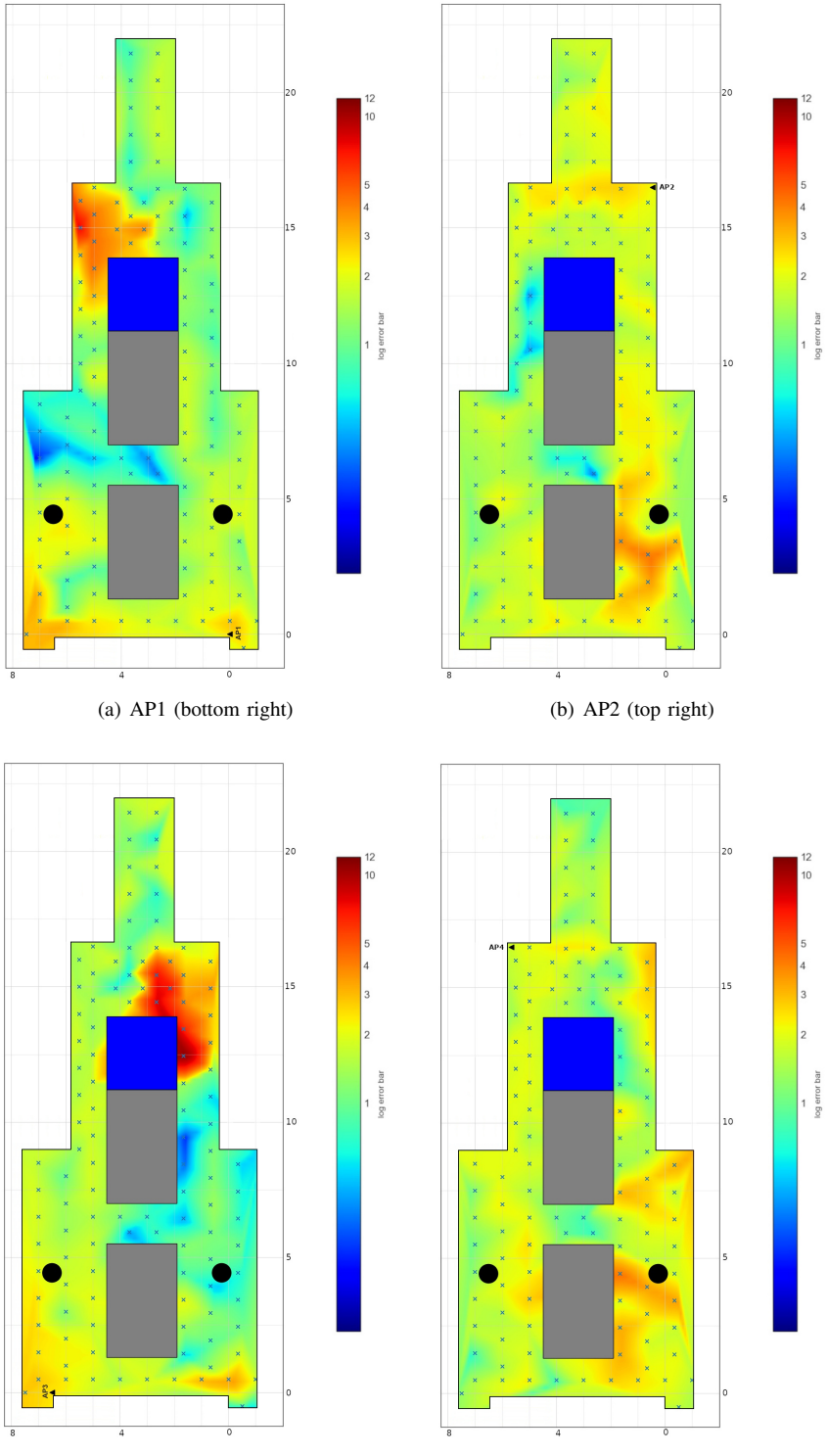

(a) AP1 (bottom right)

(b) AP2 (top right)

(c) AP3 (bottom left)

(d) AP4 (top left)

Fig. 5. Error of the estimated distance to each AP at each reference point (averaged over the 4 STA orientations).

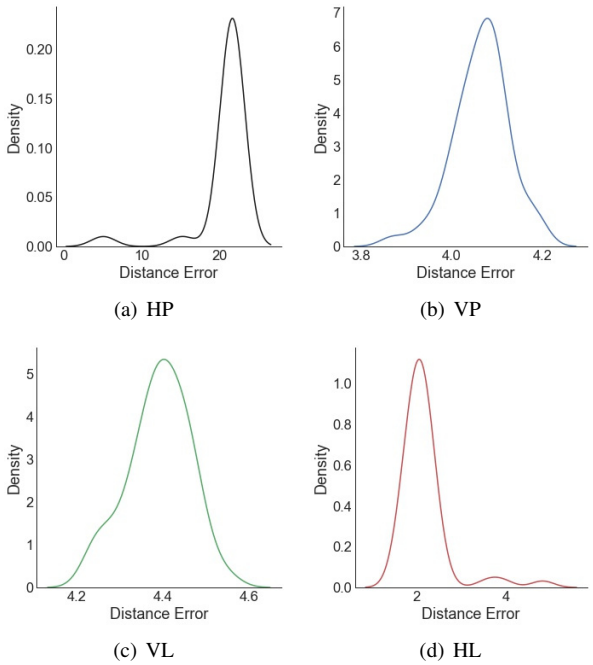

Fig. 6. Probability Density Function of the Absolute Distance Error (in meters) in observations from RP (15, 5.5) to AP1 and for the 4 STA orientations.

tends previous analysis in [4], where only LOS conditions were studied. Four APs are located in the corners of our scenario. Samples from these APs have been collected in 117 reference points that are located in an asymmetric way along the scenario, so to avoid possible bias in the measurements observed at the APs. Four different STA orientations have been used in order to assess its impact on the ranging error.

As a general observation, very different behaviors are recorded, depending on the STA orientation. On the one hand, the HP orientation always shows the highest errors for all the APs. On the other hand, the landscape orientation of the STA seems to perform better on the overall, with a 90th percentile of the mean absolute error always lower than 2.73 m for all the APs. Also, despite the NLOS conditions of the studied scenario, the 90th percentile of the absolute error averaged over 1 meter is lower than 2.5 m for actual distances up to 13 m, again when the STA is held as landscape.

It has also been observed that the geometry of the walls may allow for constructive reflections of the signal, thus improving the ranging accuracy in NLOS areas; on the other hand, the obstruction of "hard obstacles" (e.g., concrete columns or metal objects like the elevator) greatly affects the accuracy of this ranging solution. In the latter conditions, other techniques should be investigated and applied to improve the accuracy of the ranging technique. This aspect is out of the scope of this paper and is left for future research. However, it should be noted that, depending on the positioning technique used to gather a position from this ranging estimations, this bias may not constitute a problem (i.e., fingerprinting).

ACKNOWLEDGMENT

The Article Processing Charges were funded by the Spanish Government and ERDF through CICYT project under grant PGC2018-099945-B-I00. This research was partially supported by PGC2018-099945-B-I00 and by the European GNSS Agency under grant GSA/GRANT/04/2019/BANSHEE.

REFERENCES

[1] Kul, G.; Özyer, T.; Tavli, B. "IEEE 802.11 WLAN based Real Time Indoor Positioning: Literature Survey and Experimental Investigations." Computer Science 2014, 34, 157–164.

[2] Yassin, A., et al. "Recent Advances in Indoor Localization: A Survey on Theoretical Approaches and Applications", IEEE Communications Surveys & Tutorials, 2017, 19, 1327-1346.

[3] Laoudias, C., et al. "A Survey of Enabling Technologies for Network Localization, Tracking, and Navigation." IEEE Communications Surveys & Tutorials. 2018, 20, 3607–3644.

[4] Martin-Escalona, I.; Zola, E. "Ranging Estimation Error in WiFi Devices Running IEEE 802.11mc," GLOBECOM 2020 - 2020 IEEE Global Communications Conference, 2020, pp. 1-7.

[5] Zafari, F.; Gkelias, A.; Leung, K.K. "A Survey of Indoor Localization Systems and Technologies." IEEE Communications Surveys & Tutorials, 2019, vol. 21, no. 3, pp. 2568-2599.

[6] Majeed, K., et al. "Indoor Localization and Radio Map Estimation Using Unsupervised Manifold Alignment with Geometry Perturbation." IEEE Transactions on Mobile Computing, vol. 15, no. 11, pp. 2794-2808, 1 Nov. 2016.

[7] Ciurana, M.; Barcelo, F.; Izquierdo, F. "A ranging system with IEEE 802.11 data frames," in Proc. IEEE RWS'07, Jan. 2007.

[8] Hoene, C.; Willmann, J. "Four-way TOA and software-based trilateration of IEEE 802.11 devices." In Proc. of the IEEE 19th Int. Symposium on Personal, Indoor and Mobile Radio Communications, Cannes, France, 15–18 September 2008; pp. 1–6.

[9] Martin-Escalona, I.; Barcelo-Arroyo, F.; Zola, E. "A software platform for measuring distances through round trip time in IEEE 802.11." In Proceedings of the IEEE Wireless and Mobile Networking Conference (WMNC), Dubai, UAE, 23–25 April 2013; pp. 1–4.

[10] IEEE Standard for Information technology. Telecommunications and information exchange between systems Local and metropolitan area networks. Specific requirements - Part 11: Wireless LAN Medium Access Control (MAC) and Physical Layer (PHY) Specifications," in IEEE Std 802.11-2016 (Revision of IEEE Std 802.11-2012), pp.1-3534, 14 Dec. 2016.

[11] Google, "Wi-Fi RTT (IEEE 802.11mc)," 2019. Available online: https://source.android.com/devices/tech/connect/wifi-rtt. Last accessed June 2021.

[12] Guo, G., et al. "Indoor Smartphone Localization: A Hybrid WiFi RTT-RSS Ranging Approach," in IEEE Access, vol. 7, pp. 176767-176781, 2019.

[13] M. Si, et al. "A Wi-Fi FTM-Based Indoor Positioning Method with LOS/NLOS Identification". in Applied Sciences vol. 10, num 3:956. 2020.

[14] Google, "Nest WiFi," 2019. Available online: https://store.google.com/product/nest_wifi_specs (last accessed June, 2021).

[15] Choi, J.; Choi, Y.; Talwar, S. "Unsupervised Learning Techniques for Trilateration: From Theory to Android APP Implementation," in IEEE Access, vol. 7, pp. 134525-134538, 2019.